Journal of Marine Science and Technology

Volume 21
Issue 7 *Vol 22, Supplemental*

Article 15

DECADAL VARIATION OF WINTERTIME SEA SURFACE TEMPERATURE IN THE TAIWAN STRAIT

Yi-Chun Kuo
Department of Environmental Biology and Fishery Science, National Taiwan Ocean University, Keelung, Taiwan, R.O.C.

Ming-An Lee
Department of Environmental Biology and Fishery Science, National Taiwan Ocean University, Keelung, Taiwan, R.O.C.
Center of Excellence for Oceans, National Taiwan Ocean University, Keelung, Taiwan, R.O.C., malee@mail.ntou.edu.tw

DECADAL VARIATION OF WINTERTIME SEA SURFACE TEMPERATURE IN THE TAIWAN STRAIT

Acknowledgements

This study was part of Taiwan Integrated research program on Climate Change Adaptation Technology (TaiCCAT), sponsored by the grants from the National Science Council of Taiwan, NSC101-2625-M-019-006 and 102-2811-M-019-001.

Journal of Marine Science and Technology, Vol. 21, Suppl., pp. 117-123 (2013)
DOI: 10.6119/JMST-013-1219-9

DECADAL VARIATION OF WINTERTIME SEA SURFACE TEMPERATURE IN THE TAIWAN STRAIT

Yi-Chun Kuo[1] and Ming-An Lee[1, 2]

Key words: Taiwan Strait, Empirical Orthogonal Function, SST warming, ENSO.

ABSTRACT

Long-term advanced very-high-resolution radiometer (AVHRR) data with a resolution of 0.04° provided clearer views of sea surface temperature (SST) warming and variation associated with ENSO in the Taiwan Strait (TS) during wintertime (1981-2013). Over the 33 year period, the spatial average of winter SST warming in the TS reached to 3°C. From 1981-2001, the SST exhibited an increasing trend, with the fastest warming taking place from 1991-2001 after which it seemed to pause. From 2002-2012, the SST showed a cooling trend (-0.08°C/yr). Spatial variation of the warming was distinct, with the highest values concentrated in the winter fronts region, formed by the cold China Coastal Current (CCC) and the warm Kuroshio Branch (KB), indicating northwestward movements of the winter fronts. Influence of ENSO events on winter SST was significant, with higher SST in the CCC region in El Niño years. Temporal SST EOF results in modes 1 and 2 show a long-term warming trend and interannual variations, respectively. Consequently, the combined impacts of global ocean warming and climate variability in future will result in increasing the uncertain of SST variability in the TS.

I. INTRODUCTION

The Taiwan Strait (TS) connects the East China Sea (ECS) and the South China Sea (SCS). Water in the TS mainly flows northward owing to the pressure gradient associated with large scale circulation [6, 7]. Except in wintertime, northeasterly monsoon winds drive the cold China Costal Current (CCC) to flow southward along the west coast of the TS, while the warm Kuroshio Branch (KB) current enters the TS through the Penghu Channel from the southeast [13]. A distinct topography- the Chang-Yun Rise (CYR) (Fig. 1) - in the middle of the strait acts to constrict northward or southward water transport. The combined effect of the CYR and northeasterly winter monsoon leads to the formation of a quasi-permanent front around the northern end of the CYR [3, 12]. The horizontal temperature structure in wintertime is important because it reveals the advective redistribution of heat between the ECS and SCS; moreover, the movement of isotherms and the location of the front are crucial to local fishing grounds and the distribution of fish species [5].

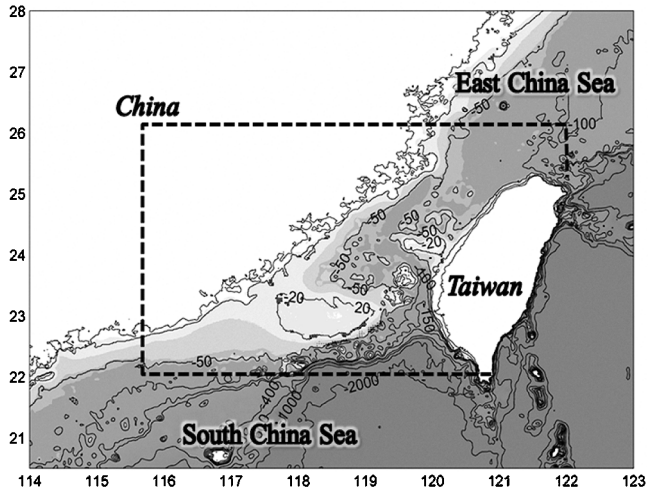

Fig. 1. Water depth (m) of the Taiwan Strait and the surrounding seas. The dotted lines mark the study region.

On interannual scales, the winter SST in the TS is influenced by the large-scale climate variability originating from the Tropical Pacific–El Niño-Southern Oscillation (ENSO) through the anomalous monsoon. It had been reported that winter SST in the TS is colder in the northwestern part and warmer in the southeastern region during a La Niña period (1998/1999), while the influence reversed during an El Niño period (1997/1998) [15]. The impact of SST variation relating to ENSO was also reflected by the catch per unit effort (CPUE) of larval anchovies [11]. In addition to this climate

Paper submitted 10/18/13; revised 12/11/13; accepted 12/19/13. Author for correspondence: Ming-An Lee (e-mail: malee@mail.ntou.edu.tw).
[1]Department of Environmental Biology and Fishery Science, National Taiwan Ocean University, Keelung, Taiwan, R.O.C.
[2]Center of Excellence for Oceans, National Taiwan Ocean University, Keelung, Taiwan, R.O.C.

variability, global ocean warming has also been identified as an important area of study in the ESC and SCS area. Belkin [2] found a fast warming of 1.22°C between 1982 and 2006 in the ECS Large Marine Ecosystem (LME), and a median warming of 0.44°C in the SCS LME. However, ocean warming rates in the TS located between ECS and SCS remain unknown. Furthermore, the topography in the TS can modify the warming trend through topography-flow interactions. Long-term high-resolution satellite data is required to detect variation of the winter front in the TS due to ocean warming trends.

In this paper, 33 years of satellite SST data with a high resolution of 4 km is used to investigate warming in the TS. Empirical Orthogonal Functions (EOF) analysis was applied to simplify and quantify the spatial and temporal SST variability. Section 2 briefly introduces the satellite data; Section 3 presents results of the data analysis; Section 4 discusses the results and presents concluding remarks.

II. DATA AND METHOD

Daily satellite SST images were collected from advanced very-high-resolution radiometer (AVHRR) sensors on NOAA satellites from December 1980 to February 2013 (http://www.class.ngdc.noaa.gov), and the regional AVHRR data library at the National Taiwan Ocean University (NTOU), Keelung, Taiwan. Navigation and cloud detection techniques were adopted from Sakaida and Kawamura [23]. The Multichannel Sea Surface Temperature (MCSST) algorithm [18] was used to produce the SST images at a spatial resolution of 4 km (1980-1995) and 1.1 km (1996-2013). Lee *et al*. [16] validated the SST algorithm by comparing the AVHRR-based MCSSTs during 1998-2002 with the in situ data. The MCSST were found to have small biases of 0.009°C with root mean square deviations of 0.64°C. The present study only used data from the winter months (December-February). The monthly SST data were formed by arithmetically averaging all available scenes in each month on a pixel by pixel basis (excluding missing data and clouds). To unify the data resolution, grids of the data for 1996-2013 were merged to a 4km x4km grid. In this way, 33 years of monthly SST data in a domain bounded between 115-122°E and 22-26°N with 154173 spatial data points can be used to study changes of winter SST patterns in the TS in response to global warming trends and other climatic variations.

EOF analysis is a statistical method used to decompose a multivariate data set into its principal components. Satellite SST data in the EOF analysis were arranged in a two-dimensional array, an $M \times N$ matrix, $T(x, t)$, where M is the number of elements in the spatial dimension, and N is the number of elements in the temporal dimension. To extract more detailed information, the temporal means were removed to reveal features that vary strongly in time [21]. The EOF modes are the eigenvectors of the covariance matrix of T, i.e. T^TT, represents time averages of covariance between data at various spatial locations. The covariance matrix was decomposed using the singular-value decomposition (SVD) method. T^TT can be represented with VS^2V^T, the singular values(S) represent the eigenvalues and eigenvectors V represent the empirical orthogonal modes. The spatial patterns and time-series variations of SSTs in the eastern TS can then be elucidated [Emery and Thomson 2001]. Using this method, the bulk of variance of a data set can be described by a few orthogonal modes and the corresponding time variation amplitude, so that the major properties of the data set can be more easily understood.

III. RESULTS

1. Decadal Variations

Fig. 2(a) shows the 33-year mean of winter SST (Dec-Feb). The red arrow points to the most significant winter front formed by the southward extension of CCC and the northward transport of the KB and SCS water [3]. According to Chang *et al*. [3], another important winter front occurs on the Taiwan Bank, which can also be seen by the squeezed isotherms in Fig. 2(a) (the blue arrow). Figs. 2(b)-(d) respectively show the 11-year average of winter SST patterns for 1981-1991, 1992-2002 and 2003-2013. On decadal scale, the entire TS was warming during 1981-2013. The 20°C isotherm (thick black lines) is chosen as an index for the winter thermal front boundary of CCC and KB in the TS [17] to represent the confinement of KB by the intrusion of cold CCC. The 20°C isotherm shows a northward movement, with its northern bound moving from 24°N to 25°N off the northwest coast of Taiwan. Meanwhile, the northward movement of the 20°C isotherm on the southwestern TS is slower than that on the eastern side (around the CYR), possibly as a result of the influence of topography. This is discussed later in this paper.

Fig. 3 shows annual variation of mean SST in the TS and its normalized pattern. The warming trend is obvious; however, the warming rate seems to have stopped in the last 10 years. Using linear regression, the warming trend of the mean pattern over 33 years is 0.1°C/yr. Fig. 3 also plots linear trends for the three periods, 1981-1991, 1992-2002 and 2003-2013. The warming rate during 1981-1991 is 0.19°C/yr. The fastest warming rate occurred during 1992-2002, reaching to a value of 0.21°C/yr. In the third time period, the SST exhibited a weak cooling trend with a rate of -0.08°C/yr.

To further observe spatial variations of SST warming, Fig. 4 plots the horizontal distribution of the linear warming rate during 1981-2013. As seen in Fig. 2, the most significant warming region is around the winter fronts extending from the northwest of the CYR to the southern Taiwan Bank. In the southeastern TS, occupied mostly by the KB, the warming is less significant (0.04°C/yr.) as compared to that in the northeastern TS (0.12-0.16°C/yr.). Along the China coast, where the CCC flows in winter, the warming rate is also small, similar to that in the southeastern region. Given the relatively low warming rates in the CCC and KB regions of the TS, the

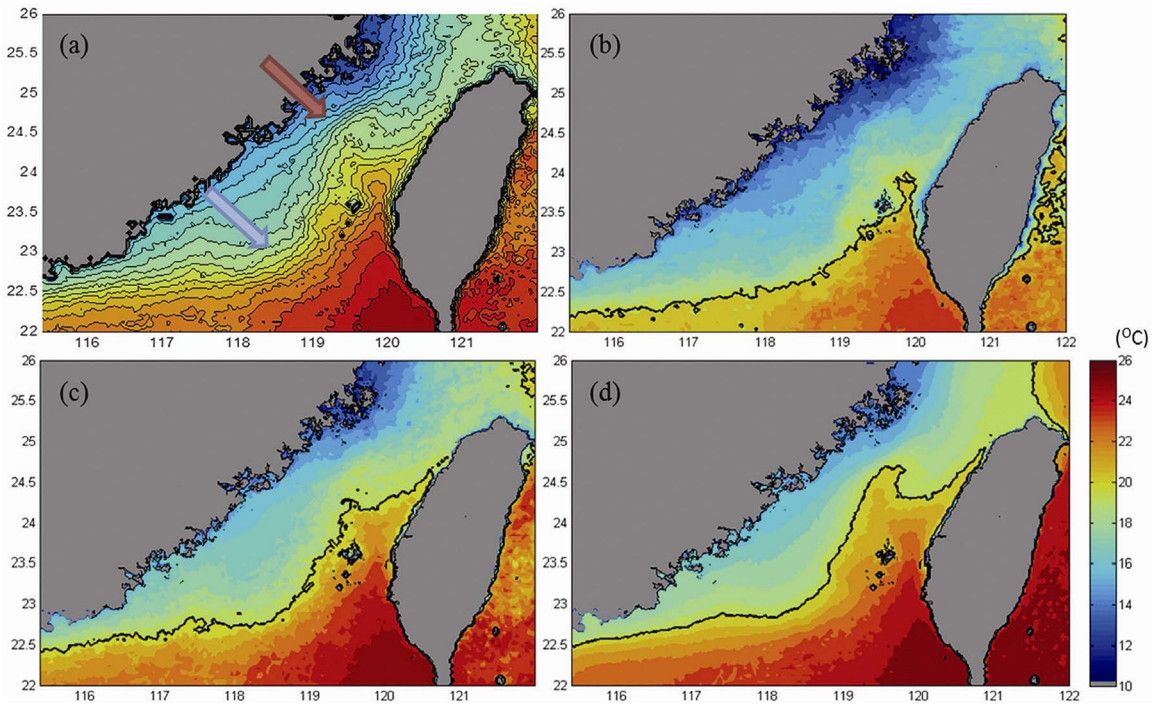

Fig. 2. (a) 33-year mean winter SST (Dec-Feb). The red and blue arrows respectively mark the Mainland China Coastal Front and the Taiwan Bank Front [3]. (b), (c) and (d) respectively plot the 11-year mean winter SST pattern for 1981-1991, 1992-2001 and 2002-2013. The thick black contours show 20°C isotherms.

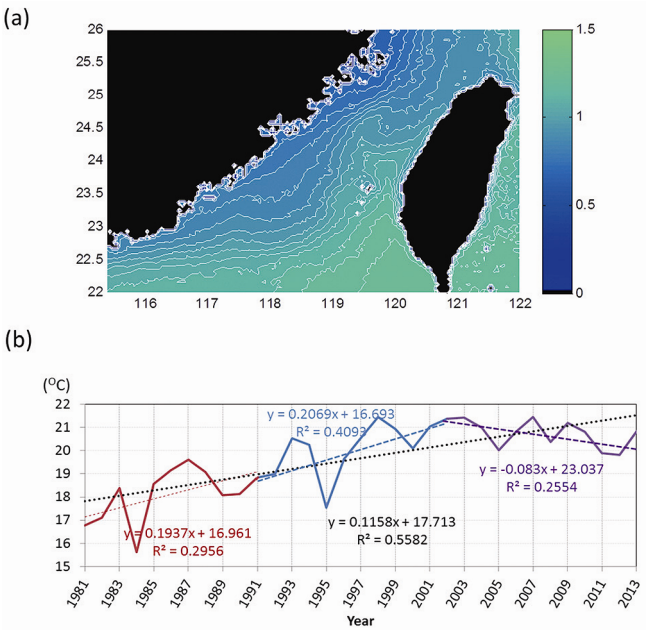

Fig. 3. (a) The mean component of winter SST and (b) its corresponding time variation. The red, blue and purple dotted lines respectively are the regression lines for 1981-1991, 1992-2002, and 2003-2013. The black line is for 1981-2013. The corresponding equations and R2 are the same colors as the regression lines.

heat source for the conspicuous warming near this winter front region was neither the warming of the ECS, SCS or Kuroshio. This particular warming could be a result of heat advection

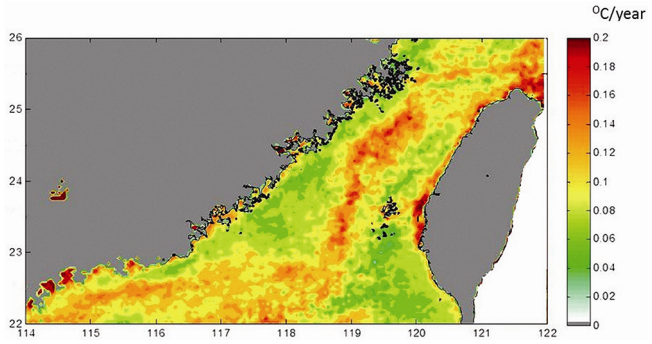

Fig. 4. Spatial distribution of the linear warming trend (°C/year) of winter SST in 1981-2013 in the TS.

by westward movement of the fronts. In other words, the KB intrusion into the northern SCS might become stronger with time.

2. Interannual Variations

Fig. 5(a) plots the winter SST variation on a transect along 23.5°N. The black line marks the 20°C isotherm. During the study period, there was a warming trend featuring a gradual northward intrusion of the 20°C isotherm; in addition, the interannual variation is conspicuous. Some yeas were exhibited significant westward movement of the warmer water (>20°C), specifically the winters of 1997-1998, 2000-2005, 2006-2007, and 2009-2010. During the winters of 1981-1982, 1983-1984 and 1994-1996, the warmer water (>20°C)

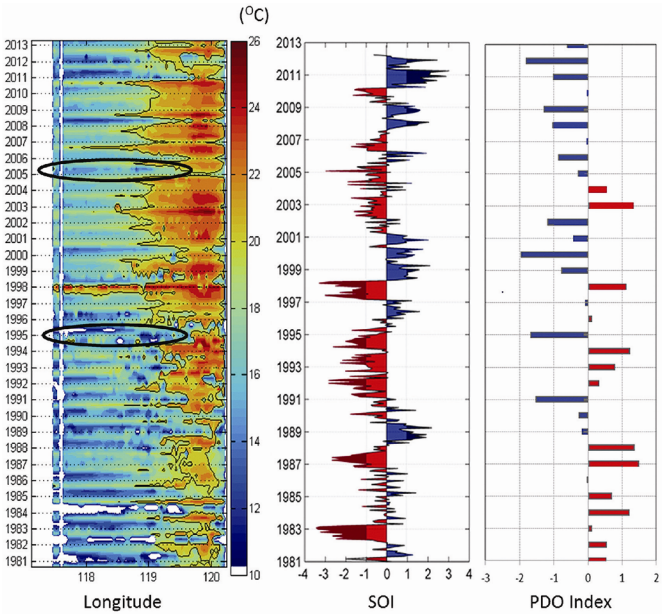

Fig. 5. (a) Winter SST variation on a transect along 23.5°N, 117°E-120.2°E. 3 months (Dec-Feb) of data were used to represent winter SST. (b) Monthly SOI index and (c) Averaged PDO index from October to December during the previous years.

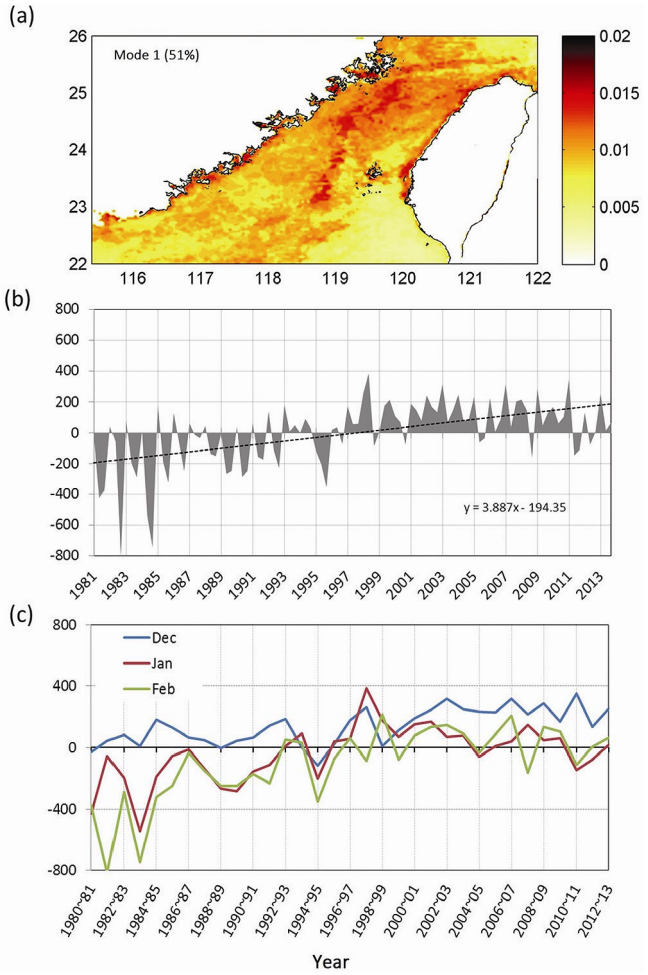

Fig. 6. (a) Spatial pattern of the EOF mode 1 and (b) its corresponding amplitude (3 month × 33 years). (c) Amplitude of each month plotted separately.

retreated east or was entirely absent in this transect. The variations seem to be coherent with the ENSO events, which are represented by the Southern Oscillation Index (SOI) which records the pressure differences between Tahiti and Darwin and is used as an indication of the intensity of El Niño (negative SOI) or La Niña (positive SOI) events (Fig. 5(b)). This result consists to the finding in Kuo and Ho [15], which revealed the SST variability associated with ENSO during 1996-2000. However, long-term observation revealed some exceptions. For example, in the winters of 1994-1995 and 2004-2005, the magnitude of the SOI index exceeds 1 (Fig. 5(b)), while the westward extent of warm water wasn't insignificant (black circles in Fig. 5(a)).

3. EOF Analysis

To further analyze the temporal and spatial variation of wintertime SST, results of the EOF analysis applied on 99 images are presented in Figs. 6 and 7. The first mode explains 51% of the total variance. It shows a spatially in-phase pattern with higher values on the northern side and along the winter fronts region. This pattern is similar to that of the warming rate shown in Fig. 4. The time series can be roughly divided into two periods. Before the winter of 1995-1996, the amplitude is mostly negative. After 1996, the amplitude is mostly positive. On decadal time scale, the increasing tendency of mode 1 amplitude is highest during 1991-2001, matching the result shown in Fig. 3. The amplitude of the first mode has an intra-seasonal cycle. To observe this monthly variation, the amplitude in December, January and February are plotted separately in Fig. 6(c). Before the winter of 1995-1996, the amplitude for January and February were negative and similar, while that for December was positive, indicating cooling from December to January. In addition, as the intrusion of the CCC was enhanced from December to January, the winter front would move southeastward. Therefore, the strongest cooling occurred near the region of the fronts. During the winter of 1994-1995, the amplitude of all three months became negative. The significant inter-annual SST variation has been attributed to the anomalous East Asia monsoon which could also cause movements of the winter fronts. After 1996, the amplitude was nearly entirely positive for all three months. In brief, the warming trend is more significant in January and February than in December. Moreover, the monthly variation in 1993-2001 seems to be smaller than in the other years.

The second mode explains 8% of the total variance, and shows a north-south out-of-phase pattern. This mode explains an opposite temperate variation of two major water sources, China coastal water and the KB water. The monthly variation is distinct (Fig. 7(c)). Generally, the amplitude of December is positive while that of January and February is negative,

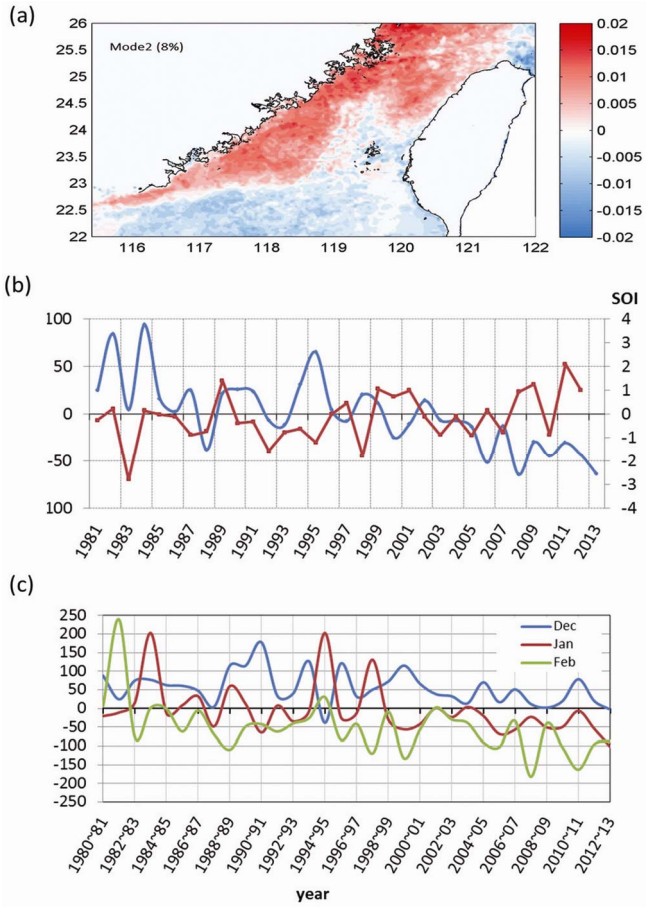

Fig. 7. (a) Spatial pattern of the EOF mode 2 and (b) its corresponding amplitude (blue line) and the SOI index (red line). (c) Amplitude of each month plotted separately.

inferring the influx of colder China coastal water and slightly warmer KB water during January and February. During wintertime the strong northerly wind pushes cold coastal water southward from China, and the northward Kuroshio branch water driven by the pressure gradient (associated with the larger circulation) will accumulate and result in downwelling due to continuity. Eventually, an anticyclonic eddy is formed south of the TS [26], thus slightly warming the southern region occurred from December to February. Fluctuation in the mode 2 amplitude is large, especially in January and February. Most of the outstanding amplitude coincides with the strong ENSO events. In Fig. 7(b), variations in the SOI time series indicate that, during times with outstanding amplitudes, the northwestern side of the TS was warmer (colder) during strong El Niño (La Niña) years. It had been reported that ENSO events can modulate the East Asia winter monsoon (EAWM). Strong (weak) northerly winds are correlated with La Niña (El Niño) [30], thus enhancing (weakening) the intrusion of the coastal current from China to the TS. From 1981 to 1999, the magnitude of negative SOI is larger than that of the positive SOI, indicating domination of El Niño events during this period. After 2000, the magnitude of negative SOI is reduced, while positive SOI became increases, especially during 2007-2012. Corresponding to this SOI tendency, the time series of the mode 2 amplitude shows a decreasing trend over the last 15 years. This trend represents variance of decreasing SST along the CCC region and increasing SST in the KB region, corresponding to the pause of warming roughly after the year 2000. Accordingly, as shown in Fig. 3, the horizontal distribution of the warming trend in the TS was slower along the CCC region.

IV. DISCUSSION

1. The TS Warming Trend

The spatial average of winter SST warming in the TS reached 3°C during 1981-2013. The warming was fastest during 1981-2000, and has slowed over the past 10 years. Wintertime circulation in the TS involves two water sources, the CCC (forming the ECS) and the KB current, both of which have exhibited SST warming over the past few decades. The rate of ocean warming in the ECS has been found to be the highest in the world [1]. In addition, the warming was stronger in winter than in other seasons [24, 25]. Zhang *et al.* [30] suggested the winter warming was related to the decreasing frequency of cold surges, which bring extremely cold and dry air from Central Asia which dissipates heat from the oceans. Oey *et al.* [19] suggested that the warming of shelf seas off the eastern coast of China in the recent decades was accompanied by stronger northeasterly wind and by on-shelf wind convergence from the open Pacific. Some recent studies used in situ data to show that the SST warming in the ECS reached 1°C/decade in May during 1959-2009 [29] and 1.96°C/decade in February during 1985-2001 [28]. On the other hand, the ocean warming of the northern SCS and the Kuroshio southeast off Taiwan was relatively mild. The differences of the warming rate between ECS and SCS might be a cause of increased warming in the northern TS during wintertime. Waters across the Strait flow northward in summer but, during wintertime, northeasterly monsoon wind can drive the CCC to flow into the TS. According to observation from NASA GISS, the global warming rate has significantly decreased during last decade, along with global SST warming. Some studies have tried to explain the recent pause of SST warming (since 2000): Outten and Esau [20] found a band of cooling that extends across mid-latitude Eurasia during the last decade, which they suggested is related to the loss of Arctic sea ice, which decreased the meridional temperature gradient and hence the large-scale atmospheric flow of the Northern Hemisphere. In the TS, the SST variation in wintertime is more complicated, the winter circulation in the TS varies with the intensity of East Asia monsoon. The cold CCC and warm KB current form a front located to the northwest of the CYR, moreover, the topographic effect plays in important role, which impedes the northward KB and causes it to turn to west.

The stronger warming rate in the region of the fronts indi-

cates its movement toward the CCC. More data is needed, such as sea surface height or in situ measurements, to determine whether the KB current transport in the TS is in an increasing trend, and which might be due to the weakening of the northeasterly winter monsoon or changes to the pressure gradient corresponding to large-scale circulation anomalies.

2. Variations Associated with Climate Variability

The ENSO event can affect the East Asia Winter Monsoon (EAWM) through the atmosphere–SST interaction and mid latitude–tropical interaction [27]. Furthermore, Pan *et al*. [22] found that the El Niño event caused a stronger southwesterly wind in summer and weaker northeasterly wind in winter in the northwestern Pacific. Because the growth/decline of the KB accompanying the decline/growth of the CCC in the TS is controlled mostly by the winter monsoon, the ENSO effect might explain part of the interannual variability seen in Fig. 5(a). In addition to the ENSO index associated with the SST anomaly in the tropical Pacific, wind speed and wind duration were found to be important factors. Chang *et al*. [5] found that the CCC intrusion was significant only when wind speed >6m/s for more than 8 days.

Recent studies have found that the ENSO-EAWM relationship might be attributable to the combined effect of the Pacific Decadal Oscillation (PDO) [10, 14]. The ENSO and PDO have similar spatial structures. Generally, the positive/negative PDO period is more likely to coincide with El Niño/La Niña. Still, there are some El Niño/La Niña years in the negative/positive PDO period. However, the ENSO signals are strongest in the tropics while the PDO features are most visible in the North Pacific [9]. Kim *et al*. [15] reported that when PDO and ENSO are in an in-phase combination (i.e., El Niño/positive PDO or La Niña/negative PDO) during wintertime with high pressure and warm sea surface temperature anomalies, the anticyclone over the western North Pacific, including the East Asian marginal seas, will significantly strengthen (weaken) during El Niño (La Niña) years, leading to suppression (reinforcement) of the EAWM. On the other hand, when PDO and ENSO are out of phase, the influence of ENSO on the EAWM would be much weaker. During the previously mentioned 'exception winters' (black circles in Fig. 5(a)) with warming and cooling in the La Niña and El Niño periods, respectively, the ENSO and PDO index are in an out-of-phase situation (Figs. 5(b) and 5(c)). These might explain these unexpected SST variations.

V. CONCLUSION

High resolution AVHRR satellite data provides a clearer view of wintertime SST warming and its variation associated with ENSO in the TS. Moreover, the spatial variation of the warming was distinct, with a higher value in the winter fronts region, indicating westward movements of the winter fronts.

The warming rate in the TS during 1981-2013 could be divided into 3 stages. The mean pattern of SST showed an increasing trend from 1981-2000, with the highest warming rate occurring during 1990-2000, with a value of 0.21°C/yr., after which it seemed to pause, from 2002-2012, the SST shows a cooling trend (-0.08°C/yr.). Spatial variation of the warming was distinct, with the highest values concentrated in the winter fronts region, formed by the CCC and the Kuroshio Branch, indicating northwestward movements of the winter fronts. The ENSO events had a significant impact on winter SST, with an average SST on the northern side of the TS in the El Niño years 2°C higher than in the La Niña years. In the El Niño years, the summer southwesterly was usually stronger and the winter northeasterly was usually weaker, thus northward intrusion of the KB and the South China Sea Current into the TS were enhanced. The weaker winter northeasterly wind couldn't sufficiently drive the CCC southward. In the La Niño years, the situation was the opposite, the CCC could intrude farther south.

Overall, the combined impact of global ocean warming and the ENSO results in increasing wintertime SST variability in the TS and marine ecosystems. More surveys in this area and studies with climate prediction models are needed.

ACKNOWLEDGMENTS

This study was part of Taiwan Integrated research program on Climate Change Adaptation Technology (TaiCCAT), sponsored by the grants from the National Science Council of Taiwan, NSC101-2625-M-019-006 and 102-2811-M-019-001.

REFERENCES

1. Belkin, I., Krishfield, R., and Honjo, S., "Decadal variability of the North Pacific Polar Front: Subsurface warming versus surface cooling," *Geophysical Research Letters*, Vol. 29, DOI: 10.1029/2001GL013806 (2002).
2. Belkin, I. M., "Rapid warming of Large Marine Ecosystems," *Progress in Oceanography*, Vol. 81, pp. 207-213 (2009).
3. Chang, Y., Shimada, T., Lee, M. A., Lu, H. J., Sakaida, F., and Kawamura, H., "Wintertime sea surface temperature fronts in the Taiwan Strait," *Geophysical Research Letters*, Vol. 33, L23603 (2006).
4. Chang, Y., Lee, K. T., Lee, M. A., and Lan, K. W., "Satellite observation on the exceptional intrusion of cold water in the Taiwan Strait," *Terrestrial, Atmospheric and Oceanic Sciences*, Vol. 20, pp. 661-669, DOI: 10.3319/TAO.2008.08.07.01(Oc) (2009).
5. Chang, Y., Lee, M. A., Lee, K. T., and Shao, K. T., "Adaptation of fisheries and mariculture management to extreme oceanic environmental changes and climate variability in Taiwan," *Marine Policy*, Vol. 38, pp. 476-482 (2013).
6. Chuang, W.-S., "Dynamics of subtidal flow in the Taiwan Strait," *Journal of the Oceanographical Society of Japan*, Vol. 41, pp. 65-72 (1985).
7. Chuang, W.-S., "A note on the driving mechanisms of current in the Taiwan Strait," *Journal of the Oceanographical Society of Japan*, Vol. 42, pp. 355-361 (1986).
8. Emery, W. J. and Thomson, R. E., *Data Analysis Methods in Physical Oceanography*, Elsevier, pp. 319-343 (2001).
9. Hare, S. R., Mantua, N. J., and Francis, R. C., "Inverse production regimes: Alaska and west coast Pacific salmon," *Fisheries*, Vol. 24, pp. 6-14 (1999).
10. He, S. and Wang, H., "Oscillating relationship between the East Asian winter monsoon and ENSO," *Journal of Climate*, accepted (2013).
11. Hsieh, C. H., Chen, C. S., Chiu, T. S., Lee, K. T., Shieh, F. J., Pan, J. Y.,

and Lee, M. A., "Time series analyses reveal transient relationships between abundance of larval anchovy and environmental variables in the coastal waters southwest of Taiwan," *Fisheries Oceanography*, Vol. 18, pp. 102-117 (2009).
12. Jan, S., Chen C. S., and Wang, J., "A numerical study on currents in the Taiwan Strait during winter," *Terrestrial, Atmospheric and Oceanic Sciences*, Vol. 9, pp. 615-632 (1998).
13. Jan, S., Wang, J., Chern, C. S., and Chao, S. Y., "Seasonal variation of the circulation in the Taiwan Strait," *Journal of Marine System*, Vol. 35, pp. 249-268 (2002).
14. Kim, J. W., Yeh, S. W., and Chang, E. C., "Combined effect of El Niño-Southern Oscillation and Pacific Decadal Oscillation on the East Asian winter monsoon," *Climate Dynamics*, DOI: 10.1007/s00382-013-1730-z (2013).
15. Kuo, N. J. and Ho, C. R., " ENSO effect on the sea surface wind and sea surface temperature in the Taiwan Strait," *Geophysical Research Letters*, Vol. 31, L13309 (2004).
16. Lee, M. A., Chang, Y., Futoki, S., Kawamura, H., Cheng, C. H., Chan, J. W., and Huang, I., "Validation of satellite-derived sea surface temperatures for waters around Taiwan," *Terrestrial, Atmospheric and Oceanic Sciences*, Vol. 16, pp. 1189-1204 (2005).
17. Lee, M. A., Yang, Y. C., Shen, Y. L., Chang, Y., Tsai, W. S., Lan, K. W., and Kuo, Y. C., "Effects of an unusual cold-water intrusion in 2008 on sudden change in catch of the coastal fishing methods around Penghu Islands, Taiwan," *Terrestrial, Atmospheric and Oceanic Sciences*, Doi: 10.3319/TAO.2013.08.06.01(Oc) (2014). (in press)
18. McClain, E. P., Pichel, W. G., and Walton, C. C., "Comparative performance of AVHRR based multichannel sea surface temperatures," *Journal of Geophysical Research*, Vol. 90, pp. 11587-11601 (1985).
19. Oey, L. Y., Chang, M. C., Chang, Y. L., Lin, Y. C., and Xu, F. H., "Decadal warming of coastal China Seas and coupling with winter monsoon and currents," *Geophysical Research Letters*, DOI: 10.1002/2013GL058202 (2013).
20. Outten, S. D. and Esau, I., "A link between Arctic sea ice and recent cooling trends over Eurasia," *Climatic Change*, Vol. 110, pp. 1069-1075, DOI: 10.1007/s10584-011-0334-z (2012).
21. Paden, C. A., Abbott, M. R., and Winant, C. D., "Tidal and atmospheric forcing of the upper ocean in the Gulf of California: 1. Sea surface temperature variability," *Journal of Geophysical Research*, Vol. 96, pp. 18337-18359, DOI: 10.1029/91JC01597 (1991).
22. Pan, J., Yan, X.-H., Zheng, Q., Liu, W. T., and Klemas, V. V., "Interpretation of scatterometer ocean surface wind vector EOFs over the Northwestern Pacific," *Remote Sensing of Environment*, Vol. 84, pp. 53-68 (2003).
23. Sakaida, F. and Kawamura, H., "Accuracies of NOAA/NESDIS sea surface temperature estimation technique in the oceans around Japan," *Journal of Oceanography*, Vol. 48, pp. 345-351 (1992).
24. Schneider, T. and Held, I., "Discriminants of twentieth-century changes in Earth surface temperatures," *Journal of Climate*, Vol. 14, pp. 249-254, DOI: 10.1175/1520-0442(2001)014<0249:LDOTCC>2.0.CO;2 (2001).
25. Thompson, D. W. J. and Wallace, J. M., "Regional climate impacts of the Northern Hemisphere annular mode," *Science*, Vol. 293, pp. 85-89, DOI: 10.1126/science.1058958 (2001).
26. Wang, J. and Chern, C.-S., "On cold water intrusions in the eastern Taiwan Strait during the cold season," *Acta Oceanographica Taiwanica*, Vol. 22, pp. 43-67 (1989).
27. Wang, B., Wu, R., and Fu, X., "Pacific-East Asian teleconnection: How does ENSO affect East Asian climate?" *Journal of Climate*, Vol. 13, pp. 1517-1536 (2000).
28. Wang, F., Meng, Q. J., Tang, X. H., and Hu, D. X., "The long-term variability of sea surface temperature in the seas east of China in the past 40 a," *Acta Oceanologica Sinica*, Vol. 32, pp. 48-53, DOI: 10.1007/s13131-013-0288-2 (2013).
29. Xu, Z. L., Gao, Q., Kang, W., and Zhou, J., "Regional warming and decline in abundance of Euchaetaplana (Copepoda, Calanoida) in the nearshore waters of the East China Sea," *Journal of Crustacean Biology*, Vol. 33, pp. 323-331, DOI: 10.1163/1937240X-00002140 (2013).
30. Zhang, I., Sperber, K. R., and Boyle, J. S., "Climatology and interannual variation of the East Asian winter monsoon: Results from the 1979-95 NCEP/NCAR reanalysis," *Monthly Weather Review*, Vol. 125, pp. 2605-2619, DOI: 10.1175/1520-0493(1997)125<2605:CAIVOT>2.0.CO;2 (1997).